NUMERICAL STUDY ON THE IMPROVEMENT OF FLOW DISTRIBUTION UNIFORMITY AMONG PARALLEL MINICHANNELS

Pistoresi C., Fan Y., Wei M and Luo L.*
*Author for correspondence
Laboratoire de Themocinétique de Nantes, UMR CNRS 6607
Polytech' Nantes – University of Nantes,
Rue Christian Pauc, BP 50609, 44306 nantes Cedex 03,
France,
E-mail: lingai.luo@univ-nantes.fr

ABSTRACT

Parallel micro or mini-channels are widely used in various devices of process and energy engineering including micro-reactors, compact heat exchangers and fuel cells. Nevertheless, the flow maldistribution due to the improper design of distributor/collector is usually observed, leading to globally poor performances of these devices. The objective of this study is to optimize the shape of the distributor/collector pipes so as to achieve a uniform flow distribution among an array of parallel mini-channels. A Z-type ladder fluid network with 10 mini-channels in parallel having square section is introduced and investigated. Two methods are used to optimize the shape of distributor/collector pipes: a discrete stairway shape optimized according to the scaling relations proposed by Tondeur et *al.* (2011) and a continuous tapered shape with the inclined angle varying from 0° to 30°. 3D-CFD simulations are carried out using the ANSYS FLUENT code. Numerical results obtained show that a relatively uniform flow distribution may be reached by the discrete stairway shape or by the linear tapered shape under very low flow-rate conditions. Larger inclined angle or fewer channels in parallel are favorable for more uniform flow distribution under higher flow-rate conditions. Nevertheless this implies that the distributor and the collector pipes occupy a large volume so that the entire device is less compact.

NOMENCLATURE

D_h	[m]	Hydraulic diameter
e	[m]	Thickness of the fluidic network
q	[m^3.s^{-1}]	Volume flow-rate
$\overline{q}$	[m^3.s^{-1}]	Mean flow-rate among mini-channels
f	[-]	Friction factor
F	[-]	Form factor
$\vec{F}$	[kg.m.s^{-2}]	External body force
g	[m.s^{-2}]	Gravitational acceleration
I	[-]	Unit tensor
l_x	[m]	Space between two mini-channels
L	[m]	Length
MF	[-]	Maldistribution factor
N	[-]	Number of parallel mini-channels
p	[Pa]	Static pressure
R	[Pa.s.m^{-3}]	Hydraulic resistance
Re	[-]	Reynolds number
$\vec{u}$	[m.s^{-1}]	Velocity
V_{in}	[m.s^{-1}]	Velocity at the inlet of the network
w	[m]	Width
Special characters		
ΔP	[Pa]	Pressure loss
θ	[°]	Angle of Distributor/Collector pipes
μ	[kg.m^{-1}.s^{-1}]	Viscosity
Π	[-]	Stress tensor
ρ	[kg.m^{-3}]	Density of the fluid
σ	[-]	Relative flow-rate deviation
Subscripts		
c		Collector pipe
ch		Mini-channel
d		Distributor pipe
in		Inlet
k		Channel index
out		Outlet

INTRODUCTION

Chemical industries and process engineering are undergoing rapid changes in the 21st century facing the challenges of climate change and energy shortage. Process Intensification (PI) that leads to a smaller, less costly, cleaner, safer, higher productivity and more energy efficient technology is proposed as a new paradigm of process engineering (Stankiewicz and Moulijn, 2002). Particularly, the innovative design of high yield processes or compact equipments has become one of the pressing industrial needs in recent years (Commenge and Falk, 2014).

One of the routes to PI is the use of equipments with locally miniaturized structures, i.e. micro or mini-channels (Charpentier, 2005; Luo, 2013; Commenge and Falk, 2014), because of their enhanced heat and mass transfer properties. Miniaturized process and energy equipments can either be heat exchangers (e.g. Fan and Luo, 2008; Fan et *al.*, 2008; Khan and Fartaj, 2011), chemical mixers or reactors (e.g. Hessel et al., 2005; Illg et al., 2010; Guo et al., 2013), fuel cells (e.g. Sung 2006; Jackson et *al.*, 2014) or integrated multifunctional systems (e.g. Anxionnaz et *al.*, 2008; Guo et *al.*, 2014). Nevertheless, to obtain a comparable productivity with that of conventional equipment, a number of micro/mini-channels should be installed in parallel. This so-called numbering-up process is the key issue for large-scale industrial applications of miniaturized devices (Al-Rawashdeh et *al.*, 2012; Luo, 2013).

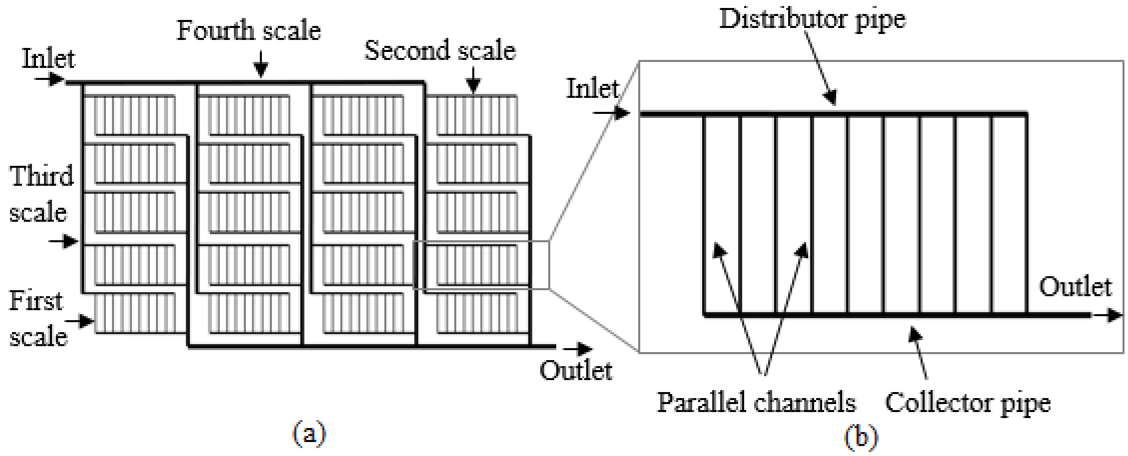

Figure 1. Multi-scale fluidic network (a) and elementary Z-type ladder circuit (b).

Therefore, the fluid distribution uniformity among the parallel channels may play an important role on the global performance of multi-channel equipments.

This is particularly true when multi-scale ladder-type fluid networks (Figure 1a) are involved (Saber et *al.* 2010; Commenge et *al.* 2011). In order to achieve uniform flow distribution among all parallel channels in the network, the first and essential step is the design of an optimized two-scale elementary Z-type ladder circuit, as shown in Figure 1b. In this elementary fluidic circuit, the single inlet port and single outlet port are located on opposite sides of the bundle of parallel cross-channels, meaning that the flow direction is the same in the distributor and the collector pipes. All cross-channels are assumed to have the same geometrical characteristics so that the passage-to-passage maldistribution may be considered as negligible (Rebrov et *al.*, 2011). On the contrary, the improper design of fluid distributor/collector pipes configuration is the main cause of flow maldistribution among the parallel cross-channels.

Many studies have then been focused on how to improve the flow distribution uniformity of the elementary Z-type ladder circuit. It is reported that a relatively uniform distribution may only be approached by making their hydraulic resistance much larger than that of the distributor and collector pipes if the latter have a uniform profile (e.g. Saber et *al.*, 2009; Tondeur et *al.*, 2011a). This usually implies that the distributor and collector pipes are large and encumbering, which is clearly unfavorable for miniaturized devices. Instead of the uniform profile (rectangular shape) of the distributor and collector, alternative shapes were proposed, such as triangular or trapezoidal-type (e.g. Kim et *al.*, 1995; Commenge et *al.*, 2002; Pan et *al.*, 2009; Renault et *al.*, 2011) or curvatured shape (e.g. Pan et *al.*, 2008; Cho et *al.*, 2010; Jackson et *al.*, 2014). In particular, Tondeur et *al.* (2011b) proposed to "taper'' the profile of distributor and collector pipes in a discrete stairway so that the flow resistances vary linearly with position, which may offer a uniform flow distribution among the parallel cross-channels. Analytical scaling relations were established based on the assumptions of Poiseuille flow and negligible singular losses (pressure losses due to divergent/convergent branching). However, the validity and the effective range of this model were never reported by numerical or experimental results.

In the present work, the flow distribution properties on a typical Z-type elemental ladder circuit are systematically investigated. We will first describe the design of discrete stairway shape distributor and collector pipes according to the scaling relations proposed by Tondeur et *al.* (2011b). In addition, a continuous model with progressive dimension reduction (or increase) for the distributor pipe (or the collector pipe) is also introduced for comparison. Then, computational fluid dynamics (CFD) simulation results for both models will be reported, under a variety of flow-rate conditions. After that influences of some design parameters including the inclined angle and the number of parallel channels will also be discussed. Finally, mains conclusions and perspectives will be summarized.

Conductive cooling of heat-generating volumes has been approached by other researchers as a volume- or area-to-point heat transfer problem [5]. Thermal tree theories have been developed to describe the distribution of low thermal resistant paths and heat transfer has been optimised for different thermal tree structures [6-8].

Even though thermal tree schemes present optimised heat transfer performance, it requires complex geometric layouts which at small dimensional scales can lead to high manufacturing costs. In passive power electronic modules, which typically have inductive, capacitive and transformative functions, restrictions imposed by the electromagnetic fields, dictates that only parallel-running internal embedded solid geometries can be considered. Such layouts, when placed in-line with magnetic field lines reduces the interference a cooling insert may have on magnetic and electric field distribution. Three-dimensional thermal path networks are thus not suitable for such applications

In a previous investigation [9], the thermal performance of a grid of discrete parallel-running rectangular solid inserts were studied and geometrically optimised in terms of fixed volume use. At the dimensional scale of interest in power electronics and electronics cooling, it was found that the geometric shape of embedded cooling inserts has a diminishing influence on thermal performance and that the fraction of volume occupied by the cooling system plays a much more dominant role [10]. With this in mind it may be appreciated that from an economic and manufacturing point of view, continuous cooling layers provides a more practical embedded conductive cooling configuration. This paper focuses on thermal characterisation of cooling layers and aims to provide some information on thermal cooling performance.

GEOMETRY AND NUMERICAL PARAMETERS

In this section, the design of distributor/collector pipes based on two models, i.e. the discrete stairway model and the continuous tapered model will be briefly described. The CFD simulation tool and the controlling parameters will be introduced as well.

Geometry of the tested mini-channel array

Figure 2a shows a representative schematic view of Z-type elemental ladder fluid circuit. The 3D fluid domain consists of 3 sections: inlet distributor pipe, parallel mini-channel array, and outlet collector pipe. For the convenience of potential fabrication, the entire fluidic circuit has identical depth (e) of 1 mm. There are 10 parallel straight channels (N=10) of identical length (L_{ch}=20 mm), having square cross-section of 1 mm in width (w_{ch}) and 1 mm in thickness (e). They are evenly spaced (l_x=2 mm) between the axis of one channel and another. For convenience of description, these mini-channels are indexed by k from 1 to N from left to right. When a pressure difference is applied between inlet and outlet to cause flow, it will passes through the distributor pipe, the parallel channels and the collector pipe subsequently to reach the outlet. The flow-rate in kth mini-channel is notated as q_k.

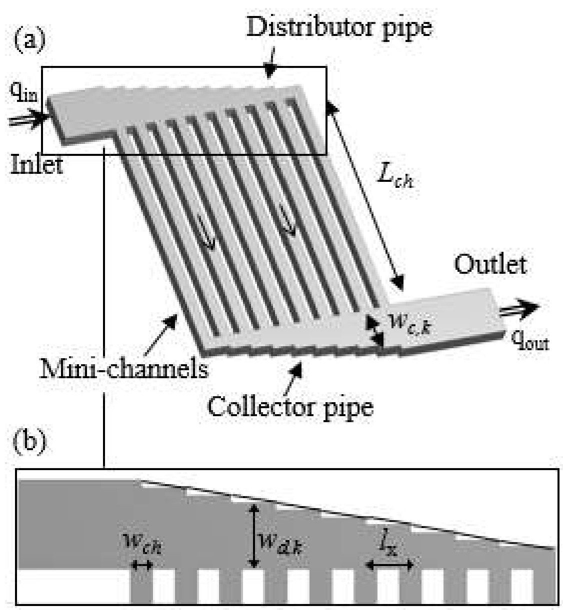

Figure 2. Z-type ladder circuit tested. (a) discrete stairway model; (b) continuous tapered model

The flow maldistribution is quantified by two parameters: the relative flow-rate deviation σ_k and the maldistribution factor MF.

$$\sigma_k = \frac{q_k - \bar{q}}{\bar{q}} \tag{1}$$

$$\mathrm{MF} = \sqrt{\frac{1}{N-1}\sum_{k=1}^{N}\left(\frac{q_k - \bar{q}}{\bar{q}}\right)^2} \tag{2}$$

where $\bar{q}$ is the mean flow-rate between parallel outlet channels. Uniform flow distribution is achieved when values of σ_k and MF approach 0.

$$\bar{q} = \frac{\sum_{k=1}^{N} q_k}{N}$$

Discrete stairway versus continuous tapered model

Tondeur et *al.* (2011b) proposed that uniform flow distribution may be approached by properly arranging the flow resistances on the segments of the distributor/collector pipes. A scaling relation was then established based on the assumption of linear flow/pressure behavior: pure Poiseuille flow, neglecting the inertial terms, neglecting or linearizing the singular effects (Tondeur et *al.* 2011b).

$$\frac{R_{d,k}}{R_{c,k}} = \frac{k}{N-k+1} \quad \text{with } k=1\ldots N \tag{4}$$

Where $R_{d,k}$ and $R_{c,k}$ are the flow resistance of kth segment of the distributor pipe or the collector pipe, respectively. Using this scaling relation, a Z-type fluid circuit with uniform cross-flow distribution can be designed. One possible example is schematically shown in Figure 3, in which the mass and pressure conservations can be easily verified.

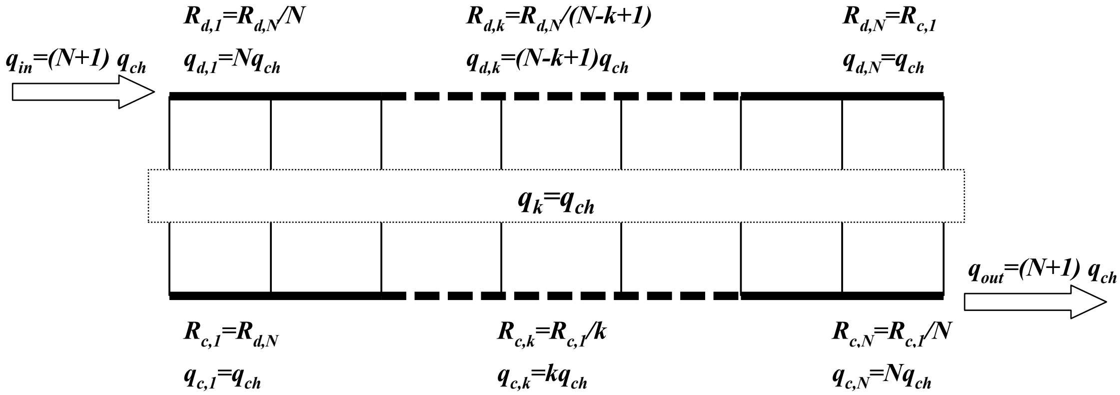

Figure 3. Flow resistance distribution for uniform flow distribution among parallel channels. Modified from Tondeur et *al.* (2011b)

The dimension of each segment of distributor/collector pipes can then be determined by supposing Poisseuille flow in straight channel with rectangular cross-section. The flow resistance in kth segment of the distributor pipe $R_{d,k}$ may be expressed as:

$$R_{d,k}=\frac{1}{2}\rho f_{d,k}\frac{L_{d,k}}{D_{h,k}ew_{d,k}}v_{d,k} \tag{5}$$

Where ρ is the density of fluid, $L_{d,k}$ the length of kth segment, e the depth of channels (1 mm), $w_{d,k}$ the width of kth segment to be determined and $v_{d,k}$ the fluid velocity in the kth segment. $D_{h,k}$ is the hydraulic diameter for rectangular cross-section and $f_{d,k}$ the friction factor for a straight channel

$$D_{h,k}=\frac{2ew_{d,k}}{e+w_{d,k}} \tag{6}$$

$$f_{d,k}=\frac{F_{d,k}}{\mathrm{Re}_{d,k}}=\frac{F_{d,k}\mu}{\rho v_{d,k}D_{h,k}} \tag{7}$$

Where Re is the Reynolds number, μ the viscosity of the fluid and $F_{d,k}$ the form factor. For rectangular cross-section, the value of form factor $F_{d,k}$ varies as a function of $e/w_{d,k}$ which may be approximatively expressed as (White, 2003):

$$F_{d,k}=-50.4\left(e/w_{d,k}\right)^3+132.7\left(e/w_{d,k}\right)^2-121.2\left(e/w_{d,k}\right)+95.7 \tag{8}$$

Regrouping Eqs.5-7, we may obtain:

$$R_{d,k}=F_{d,k}\mu L_{d,k}\frac{\left(e+w_{d,k}\right)^2}{8e^3w_{d;k}^3} \tag{9}$$

It may be verified that the flow resistances for segments of collector pipe share the same expression as Eq. 9, by replacing the subscript d with c. By setting $w_{d,N}=w_{c,1}=1$ mm, the other values of $w_{d,k}$ and $w_{c,k}$ can then be derived using Eqs. 4, 8 and 9, as listed in Table 1.

Figure 2a illustrates the discrete stairway model of the Z-type ladder fluidic circuit, designed according to the morphology presented in Figure 3. Note that a continuous tapered model may also be designed, as shown in Figure 2b, by replacing the stairs by linear profiles from point to point. It may be observed that the

$w_{d,1}$ $w_{c,10}$	$w_{d,2}$ $w_{c,9}$	$w_{d,3}$ $w_{c,8}$	$w_{d,4}$ $w_{c,7}$	$w_{d,5}$ $w_{c,6}$	$w_{d,6}$ $w_{c,5}$	$w_{d,7}$ $w_{c,4}$	$w_{d,8}$ $w_{c,3}$	$w_{d,9}$ $w_{c,2}$	$w_{d,10}$ $w_{c,1}$
4.01	3.66	3.30	2.99	2.65	2.31	1.97	1.63	1.29	1.00

Table 1. Widths for the segments of distributor/collector pipes (unit: mm)

linearization leads to an approximate trapezoidal shape for the distributor and collector, with an inclined angle (θ) of about 11.3°. This value is close to the theoretical optimal angle (10.46°) proposed by the model of Renault et *al.* (2012). Numerical tests were performed for both models, i.e. the discrete stairway model and the continuous tapered model to illustrate their flow distribution properties and the related pressure drop.

Simulation parameters

In this study, geometries and meshes were generated using different modules of ANSYS Workbench 12.1. Note that due to symmetrical character of the network in the direction of the depth, half of the body had been considered in the analysis. Fluent code V.12.1.4 was used to solve Navier-Stokes equations by finite volume methods. The equation for conservation of mass or continuity is:

$$\frac{\partial\rho}{\partial t}+\nabla\cdot(\rho\vec{u})=0 \tag{10}$$

The momentum conservation equation:

$$\frac{\partial}{\partial t}(\rho\vec{u})+\nabla\cdot(\rho\vec{u}\vec{u})=-\nabla p+\nabla\cdot(\Pi)+\rho\vec{g}+\vec{F} \tag{11}$$

Where $\vec{u}$ is the velocity, p is the static pressure, $\rho\vec{g}$ and $\vec{F}$ are the gravitational body force and external body forces, Π is the stress tensor which is given by:

$$\Pi=\mu\left[\left(\nabla\vec{u}+\nabla\vec{u}^{T}\right)-\frac{2}{3}\nabla\cdot\vec{u}I\right] \tag{12}$$

where μ is the molecular viscosity, I is the unit tensor.

Pure water at constant temperature of 293 K was chosen as working fluid (density ρ=998.29 kg.m^{-3} and viscosity μ=1.003×10^{-3} kg.m^{-1}.s^{-1}). The operational pressure was fixed at 101325 Pa. In this study, simulations were performed under steady state, incompressible and isothermal condition without heat transfer. For simplification, gravity effect and viscous heating were neglected.

Velocity inlet normal to the surface was set as the boundary condition for the inlet. Four inlet velocity conditions (V_{in}) were tested: 0.00125 m.s^{-1}; 0.0125 m.s^{-1}; 0.125 m.s^{-1} and 1.25 m.s^{-1}, corresponding to a value of mean channel Reynolds number (Re_{ch}) of 1.24, 12.49, 124.99 and 1249.97 respectively. The boundary condition of outlet was set as pressure-outlet with zero static pressure. Adiabatic wall condition was applied and no slip occurred at the wall.

Laminar flow model was used under very low velocity conditions while the k-ε RNG model was used for higher velocity conditions because micro turbulences and local vortex may exist. For the pressure-velocity coupling, standard SIMPLE method was used. For discretization, standard method was chosen for pressure and first-order upwind differentiation for momentum. The solution was considered to be converged when the flow-rate at each channel and the inlet static pressure were constant from one iteration to the next (less than 0.5% variation) and the normalized residuals were lower than the order of magnitude of 10^{-6}.

Grid independence study

A grid independence study was performed using three structured meshes with different resolutions: coarse mesh (10 segments per millimeter; 0.18 million elements); medium mesh (20 segments per millimeter; 1.65 million elements) and refined mesh (30 segments per millimeter; 5.28 million elements). Simulation results with an inlet velocity of 0.125 m.s^{-1} (mean Re_{ch}=124.99) indicated a difference of 3.7% on the inlet pressure between the coarse mesh and the refined mesh, and of 0.9% between medium mesh and refined mesh. Mass flow-rates in each mini-channel were also compared, showing a maximum difference of 2.6% between the coarse mesh and the refined mesh, and of 1.3% between the medium mesh and the refined mesh. Hence, the medium mesh was selected as a compromise between the calculation time and the precision.

SIMULATION RESULTS

Figure 4 shows the contour of velocity magnitude on the mid-depth surface (symmetry) of the Z-type ladder circuit, under different inlet velocity conditions. Simulation results for the discrete stairway model are presented on the left side of Figure 4 while those for the continuous tapered model are shown on the right side. It can be observed on Figure 4a and 4b that for relatively low inlet velocity conditions (V_{in}=0.00125 m.s^{-1}; mean Re_{ch}=1.24 and V_{in}=0.0125 m.s^{-1}; mean Re_{ch}=12.49), both models could provide a relatively uniform flow distribution among the 10 parallel mini-channels. It seems that the velocity profiles in the distributor pipe and in the collector pipe are regular and symmetric, implying that the flow patterns are rather laminar. The impact of singularity losses in converging or diverging bifurcations on the flow distribution uniformity is not significant.

On the contrary for relatively high inlet velocity conditions (V_{in}=0.125 m.s^{-1}; mean Re_{ch}=124.99 and V_{in}=1.25 m.s^{-1}; mean Re_{ch}=1249.97), flow maldistribution among parallel channels is obvious, as shown on Figure 4c and 4d. This is mainly due to the stronger *inertial force* at the higher velocity so that the fluid enters the right most channels preferentially. Dead volumes may easily be observed at the entrance zone and outside the exit port of each cross-channel. Small vortex and micro-turbulences may also be observed and the velocity profiles in the distributor and in the collector pipes are no longer symmetrical.

The increase of flow maldistribution with the increasing inlet velocity may be quantitatively shown in Figure 5, which presents the relative flow-rate deviation σ of each channel for different inlet velocity conditions. For inlet velocity V_{in}=0.0125 m.s^{-1} (mean Re_{ch}=12.49), the maximum flow-rate deviation is about 0.098 and 0.117 for discrete stairway model and for continuous tapered model, respectively, implying an acceptable flow distribution uniformity. However, the maximum value of σ rapidly increases to 0.78 (stairway model) and 0.84 (continuous model) for inlet velocity V_{in}=1.25 m.s^{-1} (mean Re_{ch}=1249.97), implying significant flow maldistribution.

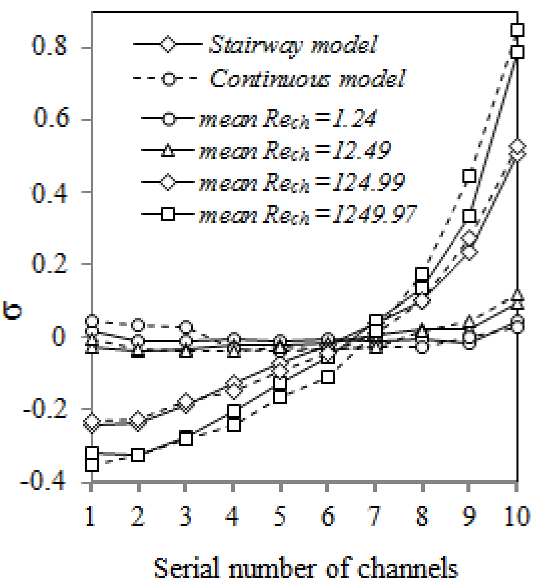

Figure 5. Relative flow-rate deviation of parallel channels for different inlet velocity conditions

Table 2 gives a comparison on the flow distribution uniformity and inlet/outlet pressure drop of the circuit between the discrete stairway model and the continuous tapered model, for different inlet velocity conditions. Very similar performances may be observed. For the same inlet velocity condition, the discrete stairway model may provide slightly better flow distribution uniformity with respect to the continuous tapered model, but generate higher pressure losses. Especially for inlet velocity V_{in}=1.25 m.s^{-1} (mean Re_{ch}=1249.97), the value of pressure loss is 5463 Pa for the discrete stairway model, 14.5% higher than that of the continuous tapered model (4616 Pa) while the values of MF are almost the same (0.38 vs. 0.39).

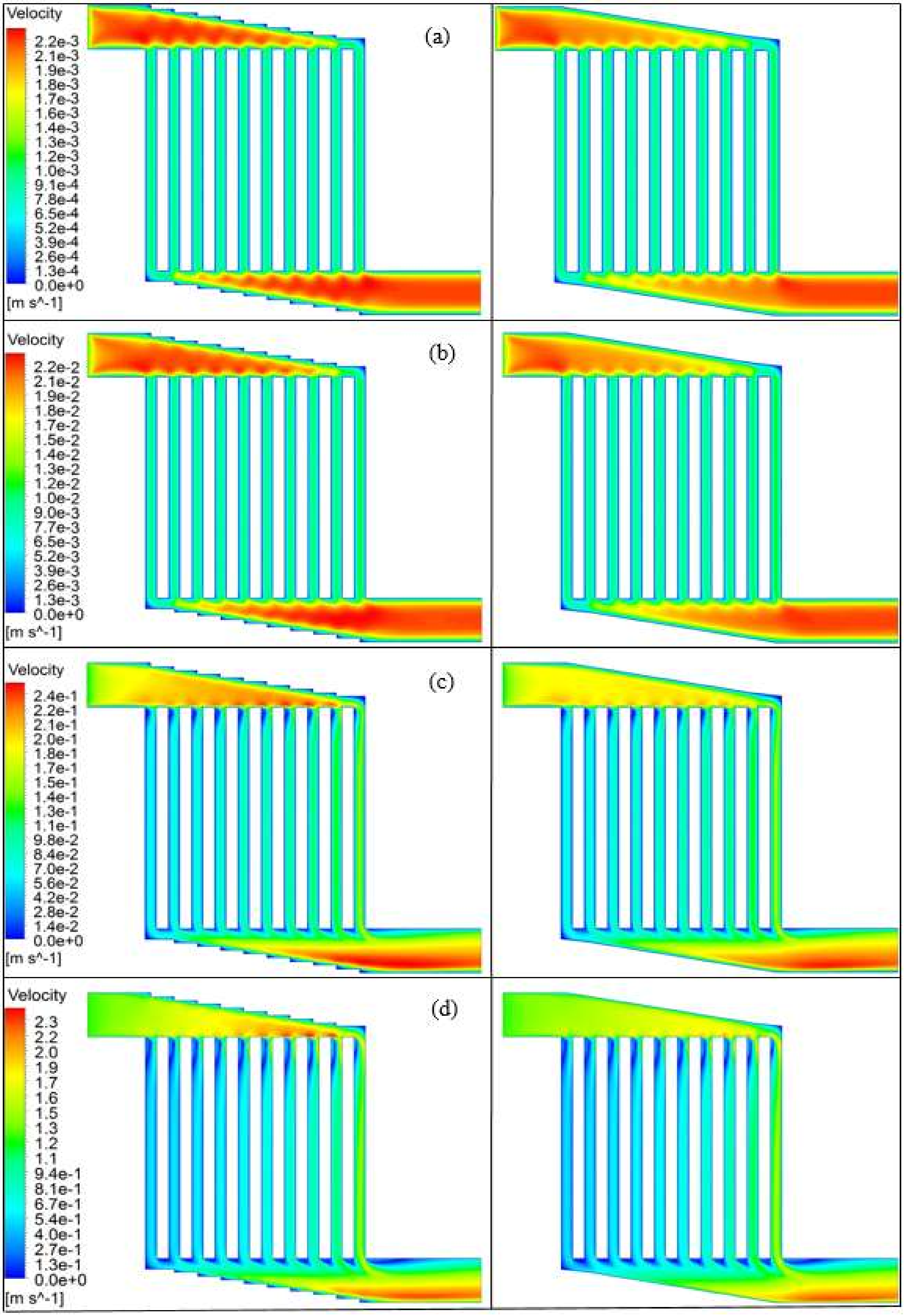

Figure 4. Velocity profiles for the discrete stairway model and for the continuous tapered model. (a) V_{in}=0.00125 m.s^{-1} (mean Re$_{ch}$=1.24); (b) V_{in}=0.0125 m.s^{-1} (mean Re$_{ch}$=12.49); (c) V_{in}=0.125 m.s^{-1} (mean Re$_{ch}$=124.99); (d) V_{in}=1.25 m.s^{-1} (mean Re$_{ch}$=1249.97)

		ΔP [Pa]		MF [-]	
Inlet velocity [m.s^{-1}]	Mean Re_{ch} [-]	Stairway	Continuous	Stairway	Continuous
0.00125	1.24	0.92	0.88	0.02	0.03
0.0125	12.49	9.48	9.05	0.04	0.05
0.125	124.99	129.64	119.66	0.23	0.24
1.25	1249.97	5463.12	4615.96	0.38	0.39

Table 2. Comparison of pressure loss (ΔP) and maldistribution factor (MF) between two models

As a short conclusion, the discrete stairway model could provide relatively uniform flow distribution only under low flow-rate conditions (e.g. V_{in}<0.0125 m.s^{-1}; mean Re_{ch}<12.49). The flow maldistribution observed at higher flow-rate conditions is mainly due to the departure from the ideal flow pattern (pure Poiseuille flow, neglecting the inertial terms, neglecting the singular effects). The continuous tapered model shows comparable performances to discrete stairway model, but may be more favorable in terms of lower pressure loss under higher flow-rate conditions. However, uniform flow distribution can no longer be guaranteed.

EFFECTS OF DESIGN PARAMETERS

In this section, the effects of some design parameters on the flow distribution uniformity will be tested and reported. We focus on the continuous tapered model because it may provide comparable flow distribution uniformity with respect to the discrete stairway model but with relatively lower pressure loss and easier to be fabricated. Two design parameters will be studied: the inclined angle (θ) of the distributor/collector pipes and the total number (N) of parallel mini-channels.

Effects of the inclined angle

Numerical simulations were performed for the Z-type ladder circuit with the inclined angle (θ) for the distributor/collector pipes varying from 0° to 30°, under four different inlet velocity conditions (mean Re_{ch} varying between 1.24 and 1249.97). The inclined angle θ=0° shows a classic rectangular shape of distributor/collector pipes while other values of θ implies a trapezoidal or near triangular shape. Other geometrical dimensions are kept as the same as the one tested in the above section.

Figure 6 shows the velocity profiles in the Z-type ladder circuit with different inclined angles for the distributor/collector pipes, for V_{in}=0.0125 m.s^{-1} (mean Re_{ch}=12.49). It may be observed that the flow always goes preferentially into the rightmost channels of the circuit, implying that at this inlet velocity, the inertial effect of fluid flow is already significant. It may also be observed that the higher the value of θ, the more uniform flow distribution may be achieved. However, this implies that the entire flow circuit becomes less compact, i.e. the distributor and collector pipes occupy a large volume.

Figure 7 indicates the influences of the inclined angle (θ) on the flow distribution uniformity of the ladder circuit, under different inlet velocity conditions. For a certain inclined angle, the flow maldistribution increases with increasing inlet velocity, as already reported before. For a same inlet velocity, larger inclined angle leads to more uniform flow distribution. However, the improvement becomes less and less notable when θ value increases. These results are in accordance with those of Pan et *al.* (2009) which said that for symmetrical manifold structures velocity distribution becomes more uniform with larger radius of inlet/outlet.

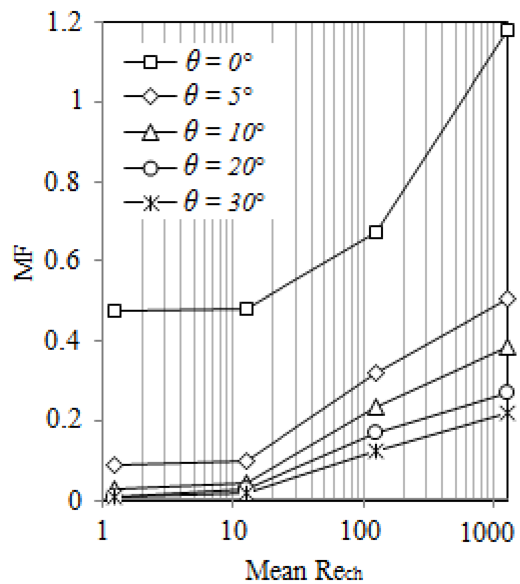

Figure 7. Influences of inclined angle on the flow distribution uniformity under different inlet velocity conditions

Influence of the number of mini-channels

3D-CFD simulations were realized on Z-type ladder circuit with number of mini-channels of 5, 10 and 20, while the inclined angle of the distributor/collector pipes was fixed at 30°, as shown in Figure 8. This is for the purpose of highlighting the influence of the number of mini-channels on the flow distribution uniformity.

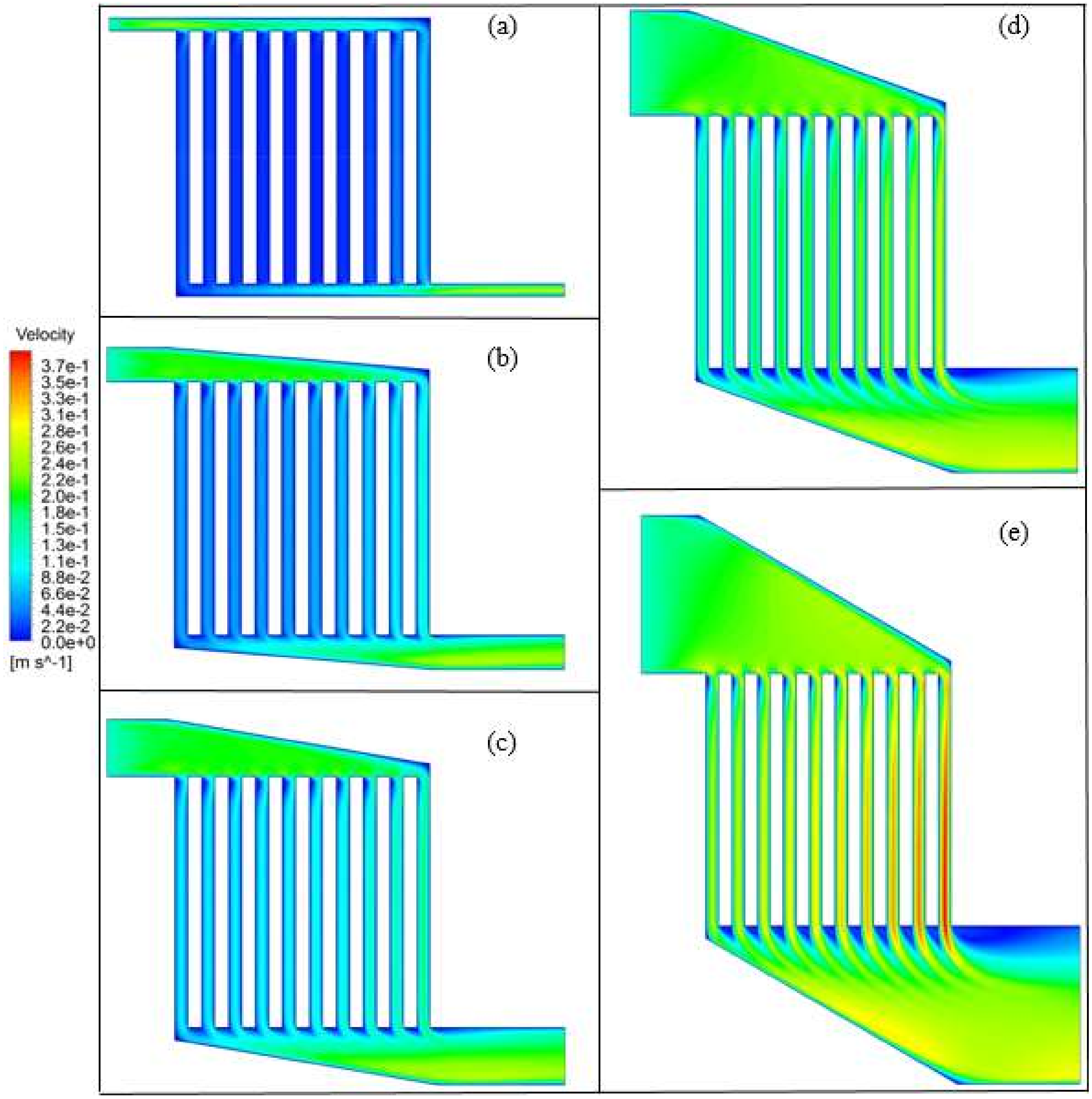

Figure 6. Velocity profiles in the Z-type ladder circuit for V_{in}=0.125 m.s^{-1} (mean Re_{ch}=124.99). (a) θ=0°; (b) θ=5°; (c) θ=10°; (d) θ=20°; (e) θ=30°

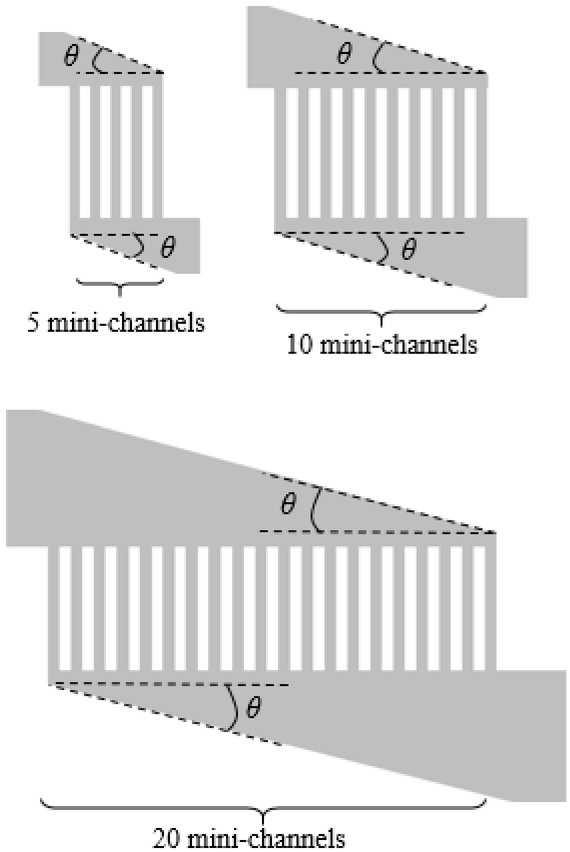

Figure 8. Geometries of ladder circuit tested with different number of mini-channels in parallel

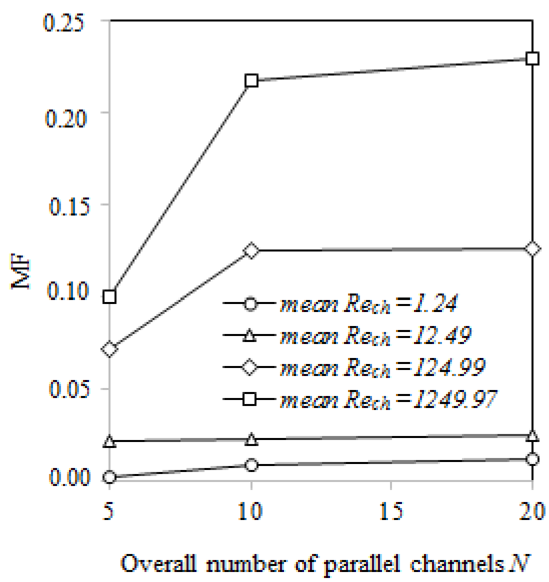

Figure 9. Influences of the number of parallel channels (N) on the flow distribution uniformity (MF) under different mean Re_{ch} conditions

Figure 9 shows the evolution of maldistribution factor as a function of the number of mini-channels under four inlet velocity conditions studied. It may be observed that the difference on the flow distribution uniformity for different N cases is relatively very small under low inlet velocity conditions (e.g. V_{in}<0. 0125 m.s^{-1}; mean Re_{ch}=12.49). However, the value of MF increases rapidly with increasing N number under high velocity conditions. For a inlet velocity V_{in}=1.25 m.s^{-1} (mean Re_{ch}=1249.97), the value of the MF increases from 0.10 for 5 channels case, to 0.217 for 10 channels case, and finally reaches 0.229 for 20 channels case. Generally speaking, it will be easier to achieve uniform flow distribution when fewer sub-streams should be formed (small N).

CONCLUSION AND PERSPECTIVES

This paper presents a numerical study on the flow distribution characteristics of a Z-type ladder circuit having 10 mini-channels in parallel. The validity and the effective range of the discrete stairway model and the continuous tapered model for the design of distributor/collector pipes are discussed. The effects of inclined angle and the number of parallel mini-channels on the distribution uniformity are also analyzed. Based on the results presented above, the following conclusions may be reached.

- The discrete stairway model could provide relatively uniform flow distribution under low flow-rate conditions (e.g. V_{in}<0.0125 m.s^{-1}; mean Re_{ch}<12.49). For higher flow-rate conditions, significant maldistribution seems inevitable.
- The continuous tapered model by linearizing the stairways may provide comparable flow distribution uniformity regarding the discrete stairway model, but may be more favorable in terms of lower pressure loss under higher flow-rate conditions.
- Increasing the inclined angle and decreasing the number of parallel channels are favorable for more uniform flow distribution. However, the compactness of the network may then be lost.

Our ongoing works are focused on the development of evolutionary algorithms (Wang et *al.*, 2010; 2014; Luo et *al.*, 2015) for more subtle modifications of the distributor/collector shape, in order to reach uniform flow distribution with small increase of pressure loss. Numerical and experimental investigations on the hydraulic and thermal characteristics of a multi-scale ladder network are also the directions of our future work.

ACKNOWLEDGEMENT

The authors would like to thank the “Region Pays de la Loire” for the project “Nouvelle équipe de recherché” and is financial support to the PhD study of M. Cyril Pistoresi.

REFERENCES

Al-Rawashdeh, M., Yu, F., Nijhuis, T.A., Rebrov, E.V., Hessel, V., Schouten, J.C., 2012, Numbered-up gas–liquid micro/milli channels reactor with modular flow distributor, Chemical Engineering Journal, 207–208, 645-655

Anxionnaz, Z., Cabassud, M., Gourdon, C., Tochon, P., 2008, Heat exchanger/reactors (HEX reactors): Concepts, technologies: State-of-the-art, Chemical Engineering and Processing: Process Intensification, 47, 2029-2050

Cho, E.S., Choi, J.W., Yoon, J.S., Kim, M.S., 2010, Modeling and simulation on the mass flow distribuion in microchannel heat sinks with non-uniform heat flux conditions, International journal of Heat and Mass Transfer 53: 1341-1348

Charpentier J.C., 2005, Process intensification by miniaturization, Chemical Engineering Technology, 28, 255-258

Commenge, J.-M., Falk, L., 2014, Methodological framework for choice of intensified equipment and development of innovative technologies, Chemical Engineering and Processing: Process Intensification, 84, 109-127

Commenge, J.-M., Falk, L., Corriou, J.P., Matlosz, M., 2002, Optimal design for flow uniformity in microchannel reactors, AIChE, 48 345-358

Commenge, J.-M., Saber, M., Falk, L., 2011, Methodology for multi-scale design of isothermal laminar flow networks, Chemical Engineering Journal, 173, 541-551

Fan, Y., Luo, L., 2008, Recent applications of advances in microchannel heat exchangers and multi-scale design optimization, Heat Transfer Engineering, 29(5): 461-474

Fan, Y., Boichot, R., Goldin, T., Luo, L., 2008, Flow distribution property of the constructal distributor and heat transfer intensification in a mini heat exchanger, AIChE Journal, 54, 2796-2808.

Guo, X., Fan, Y., Luo, L., 2013, Mixing performance assessment of a multi-channel mini heat exchanger reactor with arborescent distributor and collector, Chemical Engineering Journal, 227, 116-127

Guo, X., Fan, Y., Luo, L., 2014, Multi-channel heat exchanger-reactor using arborescent distributors: A characterization study of fluid distribution, heat exchange performance and exothermic reaction, Energy, 69, 728-741

Hessel, V., Löwe, H., Schönfeld, F., 2005, Micromixers-a review on passive and active mixing principles, Chemical Engineering Science, 60, 2479-2501

Illg, T., Löb, P., Hessel, V., 2010, Flow chemistry using milli- and microstructured reactors-From conventional to novel process windows, Bioorganic & Medicinal Chemistry, 18, 3707-3719

Jackson, J.M., Hupert, M.L., Soper, S.A., 2014, Discrete geometry optimization for reducing flow non-uniformity, asymetry, and parasitic minor loss pressure drops in Z-type configurations of fuel cells, Journal of Power Sources 269:274-283

Khan, M.G., Fartaj, A., 2011, A review on microchannel heat exchangers and potential applicaions, International journal of energy research 35:553-582

Kim, S., Choi, E., Cho, Y.I., The effect of header shapes on the flow distribution in a manifold for electronic packaging applications, International Communications in Heat and Mass Transfer 22:329-341

Luo, L., 2013, Heat & Mass Transfer Intensification and Shape Optimization: A Multi-scale Approach, Springer.

Luo, L., Wei, M., Fan, Y., Flamant, G., 2015, Heuristic shape of optimization of baffled fluid distributor for uniform flow distribution, Chemical Engineering Science, 123, 542-556

Pan, M., Tang, Y., Pan, L., Lu, L., 2008, Optimal design of complex manifold geometries for uniform flow distribution between micochannels, Chemical Engineering Journal 137:339-346

Pan, M., Zeng, D., Tang, Y., Chen, D., 2009, CFD-based study of velocity distribution among multiple parallel microchannels, Journal of Computers 4 (11), 1133-1138

Renault, C., Roche, J., Ciumag, M.R., Tzedakis, T., Colin, S., Serrano, K., Reynes, O., André-Barrès, C., Winterton, P., 2012, Design and optimization of electrochemical microreactors for continuous electrosynthesis, J App Electrochem, 42:667-677

Rebrov, E.V., Schouten, J.C., De Croon, M.H.J.M., 2011, Single-phase fluid flow distribution and heat transfer in microstructured reactors. Chemical Engineering Science, 66, 1374-1393

Saber, M., Commenge, J.-M., Falk, L., 2009, Rapid design of channel multi-scale networks with minimum flow maldistribution, Chemical Engineering and Processing: Process Intensification, 48:723-733

Saber, M., Commenge, J.-M., Falk, L., 2010, Microreactor numbering-up in multi-scale networks for industrial-scale applications: Impact of flow maldistribution on the reactor performances, Chemical Engineering Science, 65, 372-379

Stankiewicz, A., Moulijn, J.A., 2002, Process Intensification, Industrial & Engineering Chemistry Research, 41, 1920-1924

Sung, Y., 2006, Optimization of a fuel-cell manifold, Journal of Power Sources 157:395-400

Tondeur, D., Fan, Y., Commenge, J-M., Luo, L., 2011a, Flow and pressure distribution in linear discrete “ladder-type” fluidic circuits: An analytical approach, Chemical Engineering Science 66:2568-2586

Tondeur, D., Fan, Y., Commenge, J-M., Luo, L., 2011b, Uniform flows in rectangular lattice networks, Chemical Engineering Science 66:5301-5312

White, F.M., 2003, Fluid Mechanics, 5th Edition, McGraw-Hill.

Wang, L., Fan, Y., Luo, L., 2010, Heuristic optimality criterion algorithm for shape design of fluid flow. Journal of Computational Physics, 229, 8031-8044

Wang, L., Fan, Y., Luo, L., 2014, Lattice Boltzmann method for shape optimization of fluid distributor. Computers & Fluids, 94, 49-57